Surface Heat Fluxes from the NCEP/NCAR Reanalysis at the KEO Buoy Site

KUBOTA-LAB. OCEAN AND SATELLITE

○Masahisa Kubota, Noriyasu Iwabe, Meghan F. Cronin and Hiroyuki Tomita
e-mail : kubota@mercury.oi.u-tokai.ac.jp

・Background

Although the huge air-sea fluxes in the Kuroshio and Kuroshio Extension regions are easily expected to have a large impact on not only local but also global climate, until recently, continuous in situ observations of the active air-sea interaction have not been carried out because of the strong current and strong winter winds. However, in June 2004, a surface buoy, referred to as the Kuroshio Extension Observatory (KEO), was deployed by the National Oceanic and Atmospheric Administration (NOAA) in the Kuroshio Extension recirculation gyre. On the other hand, global ocean surface flux data provided by reanalysis data are widely used for various studies because of their long and consistent time series, and homogeneous spatial resolution e.g.,. ERA40 and NRA.

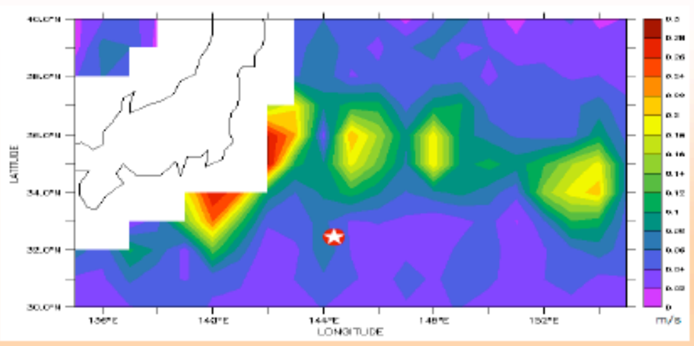

Figure 1. Location of KEO buoy

The purpose of this paper is to use data from the first deployment year of the KEO surface buoy to assess the NRA-1 and -2 heat fluxes in the Kuroshio Extension recirculation gyre. The KEO buoy is deployed at 144.5°E, 32.3°N and monitors heat, moisture and momentum fluxes, and upper ocean temperature and salinity.

・Data

The KEO buoy is essentially an enhanced Tropical Atmosphere and Ocean (TAO) buoy [e.g. McPhaden et al. 1998; Cronin et al. 2006a] modified for the severe conditions of the Kuroshio Extension region. In addition to winds, the KEO buoy measured solar and longwave radiation, rain rate, air temperature, relative humidity, and surface and subsurface temperature and salinity. Details of all sensor specifications and sampling strategies can be found on the KEO webpage: http://www.pmel.noaa.gov/keo/. Latent and sensible heat fluxes were computed from the high-resolution measurements of wind velocity, air temperature, relative humidity and sea surface temperatures using the Coupled Ocean-Atmosphere Response Experiment (COARE) bulk algorithm (Version 3.0) [Fairall et al., 2003]. Net solar radiation was computed by reducing the measured downwelling solar radiation by a factor of (1-a), where a is albedo at the ocean surface of 0.6 given by Payne(1972). We also use emissivity at the ocean surface of 0.984 for estimating upwelling longwave radiation. In this study we mainly used daily-mean data for both the buoy and NRA data for the period representing the first deployment year from July 2004 through June 2005. NRA data, with T62 spatial resolution (about 210 km), are linearly interpolated to the location of the KEO buoy using the four grid points surrounding the KEO buoy.

・Comparison of heat flux data

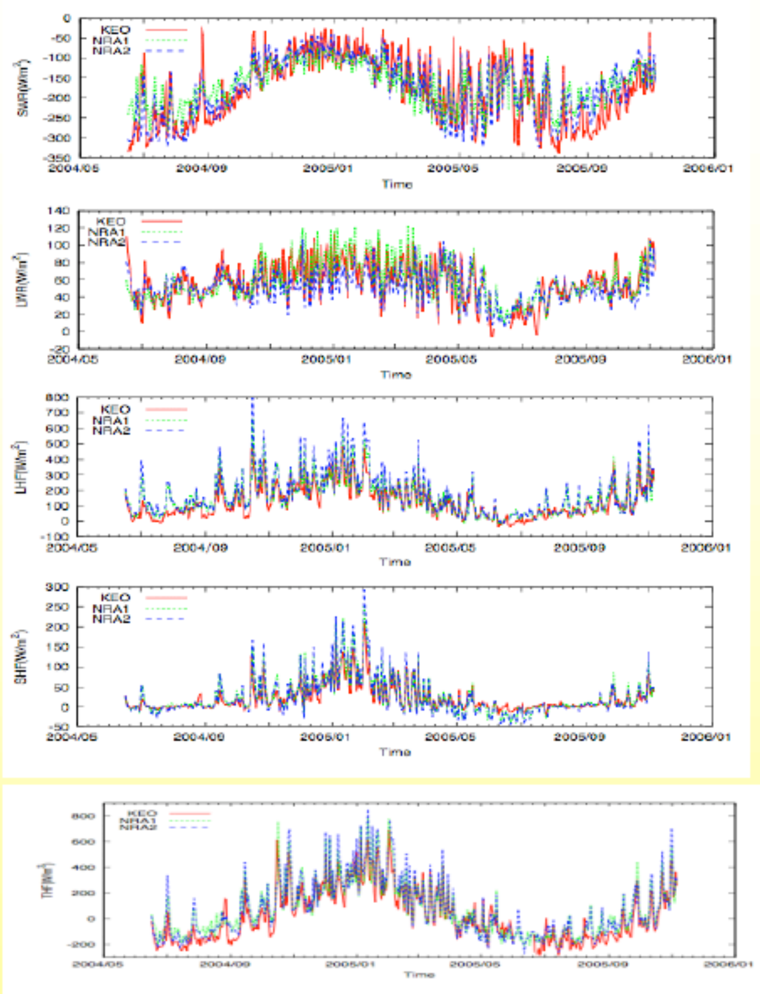

Figure 2. Time variation of each heat flux component for KEO buoy and NRA1 and NRA2 data during July 2004 and October 2005

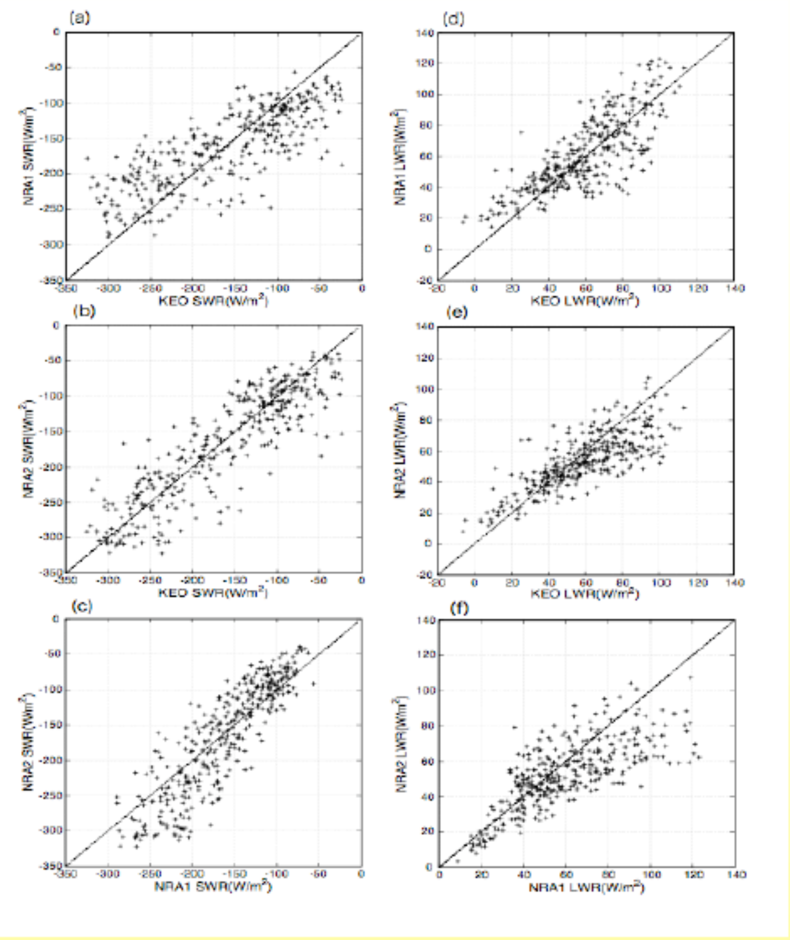

Figure 3. Scatter plots of radiation data. (a) SWR(KEO-NRA1), (b) SWR(KEO-NRA2), (c)SWR(NRA1-NRA), (d)LWR(KEO-NRA1), (e)LWR(KEO-NRA2), (f) LWR(NRA1-NRA2).

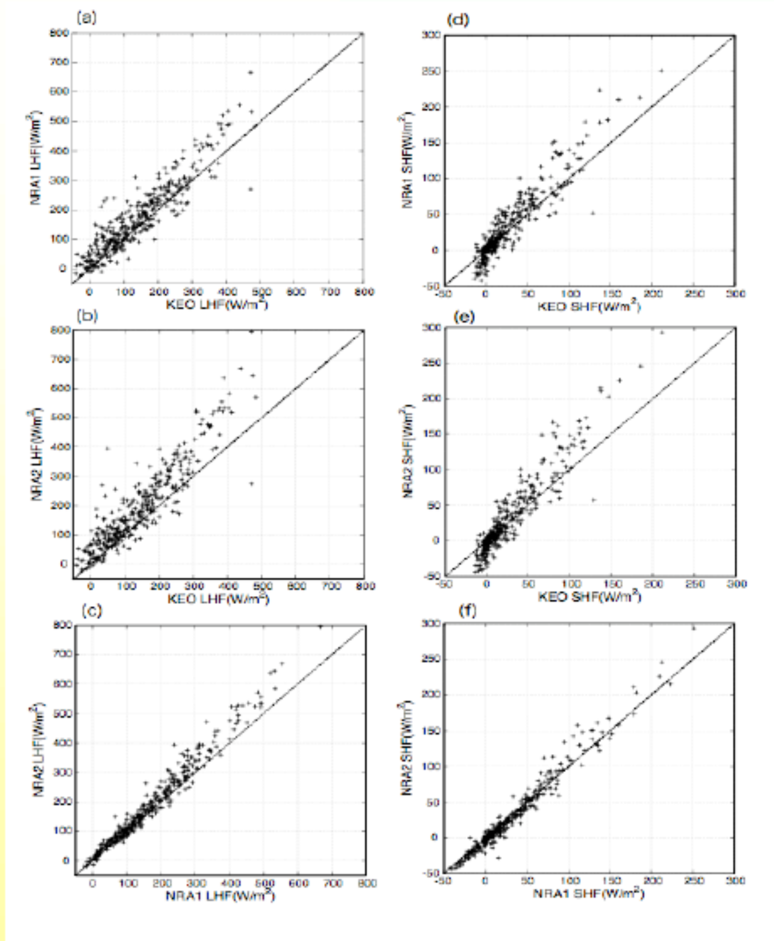

Figure 4. Same as Fig.3, except for (a) LHF(KEO-NRA1), (b) LHF(KEO-NRA2), (c) LHF(NRA1-NRA2), (d) SHF(KEO-NRA1), (e) SHF(KEO-NRA2), (f) SHF(NRA1-NRA2).

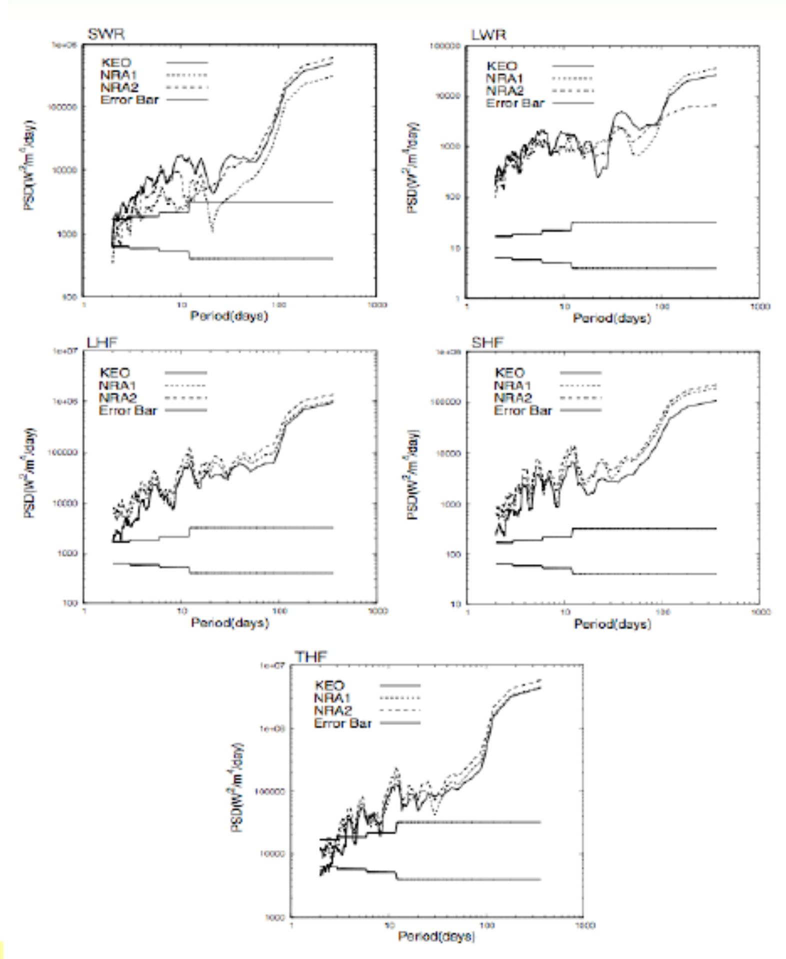

Figure 5. Power spectral density for each flux component

The NRA and KEO radiative and turbulent heat fluxes are shown in Figure 2, with positive values indicating a heat transfer from the ocean to the atmosphere. While the seasonal variations generally agree (LHF is large in boreal winter and small in boreal summer), there are some notable differences. In particular, NRA1 net shortwave radiation (SWR) data is not as large and negative as the KEO SWR data from July through September during both 2004 and 2005. Consequently, as shown in Table 1, shortwave radiation of NRA1 has a large RMS error, 51 W/m², when computed over the full first year deployment. Although the NRA-2 SWR agreement with KEO is better both in terms of the summertime and overall bias and RMS, at 39 Wm^{-2}, the NRA-2 RMS is still relatively large. Overall, as shown in the scatter plots for the radiation data (figure 3), the range of variability is much larger for solar radiation variations than for longwave radiation, and the improvement in solar radiation from NRA1 to NRA2 is larger than the slight degradation in LWR.

As shown in Figures 1 and 4, NRA turbulent heat flux data are nearly always larger than those observed by the KEO buoy, particularly during wintertime when the NRA latent (and sensible) fluxes were often more than 100 Wm^{-2} (and 50 Wm^{-2}) larger than the KEO values. The averaged latent heat flux is larger than observed by the KEO buoy by 32 Wm^{-2} for NRA-1 and by 53 Wm-2 for NRA-2 (Table 1). The values are considerably large compared with previous studies carried out for other region. We also note that TAO buoy data used in Cronin et al (2006) and Jiang et al (2005) are assimilated into NRA data. If so, this argues for the importance of using independent buoy data, such as from KEO, to assess the reanalysis data. It is concluded that the KEO site is a critical region for monitoring air-sea interactions.

As a consequence of the NRA-1 summertime bias in solar radiation and the overestimation of the turbulent heat fluxes during wintertime by both NRA-1 and NRA-2, the total heat flux out of the ocean averaged over the full year is larger than observed by the KEO buoy by 42 Wm^{-2} for NRA-1 and by 49Wm-2 for NRA-2 (Table 1). Likewise, the RMS error is about 80 W/m², for both of NRA1 and NRA2 data.

Power spectral density (PSD) of SWR for NRA1 is remarkably low compared with other data for the whole period. PSD of LWR for NRA2 appears to be quite low for periods longer than 80 days, consistent with the low annual LWR signal shown in Fig.2. The PSD for downward longwave radiation (DLWR) is not shown, however for low frequencies, the NRA1 DLWR is also lower than observed by KEO. Generally NRA turbulent heat fluxes show larger PSD than that for KEO buoy data. Because of the underestimation of shortwave radiation variability and the overestimation of turbulent heat fluxes by NRA data, the NRA and KEO total heat flux PSD agree.

Figures 2- 5 indicate that the difference between NRA1 and NRA2 fluxes is fairly large. Mean and RMS differences between NRA1 and NRA-2 are shown in Table 2. The positive average difference means that NRA1 is larger than NRA2. Average differences are positive for LWR, LHF and SHF, while average difference for SWR is negative. Therefore, NRA2 transfers smaller heat energy from the ocean to the atmosphere than NRA1.

Table 1. Correlation coefficients, RMS error, and Bias for each surface flux component of (a) NRA1 and (b) NRA2.

(a)

	SWR(W/m^2)	LWR(W/m^2)	LHF(W/m^2)	SHF(W/m^2)	THF(W/m^2)
Corr.	0.80	0.78	0.91	0.94	0.93
Rms erro	49	15	48	18	77
Bias	-3	2	32	5	42

(b)

	SWR(W/m^2)	LWR(W/m^2)	LHF(W/m^2)	SHF(W/m^2)	THF(W/m^2)
Corr.	0.88	0.78	0.90	0.94	0.94
Rms erro	38	14	60	22	82
Bias	4	-5	53	4	49

Table 2. Comparison results between NRA1 and NRA2.

	SWR(W/m^2)	LWR(W/m^2)	LHF(W/m^2)	SHF(W/m^2)	THF(W/m^2)
Corr.	0.89	0.70	0.98	0.98	0.98
Rms Diff.	38	17	31	11	49
Ave. Diff	-6	7	-21	1	-6

・Cause of the differences between KEO and NRA heat fluxes

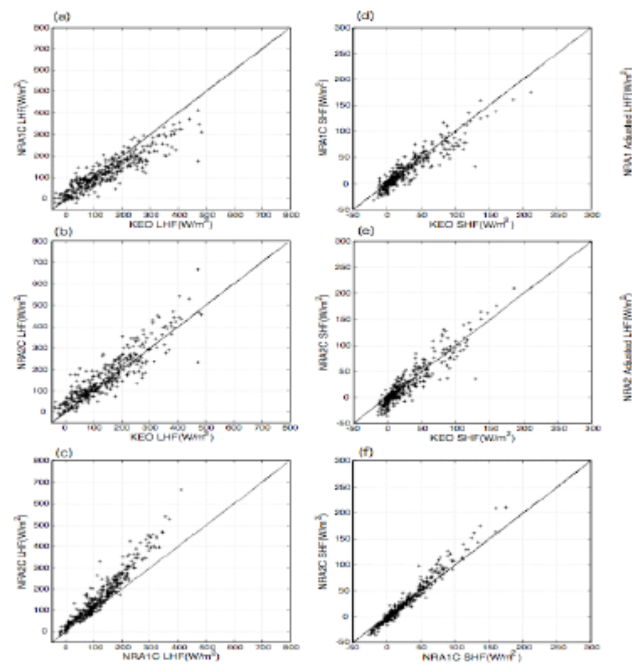

Figure 6. Same as Fig 3, except for that the turbulent heat fluxes estimated by applying CORAE 3.0 algorithm to NRA state variables. (a) LHF(KEO-NRA1C), (b) LHF(KEO-NRA2C),(c) SHF(KEO-NRA1C, (d) SHF(KEO-NRA2C).

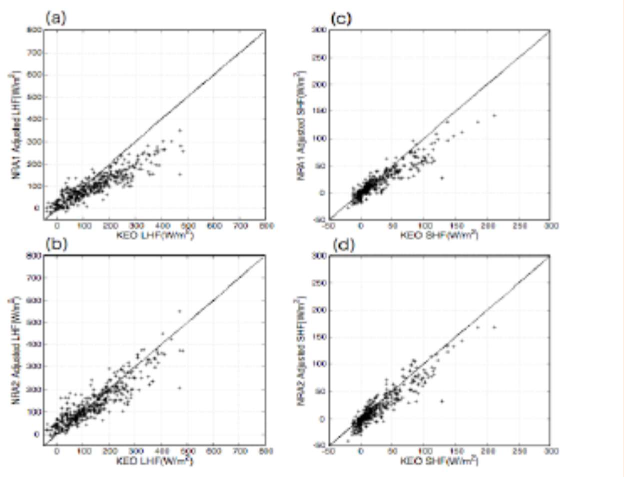

Figure 7. Same as Fig 3, except for NRA adjusted data. (a) LHF(KEO-NRA1 adjusted), (b) LHF(KEO-NRA2 adjusted),(c) SHF(KEO-NRA1 adjusted), (d) SHF(KEO-NRA2 adjusted).

Table 3. Correlation coefficients, RMS error, and Bias for turbulent heat flux component of NRA1C and NRA2C.

	LHF(W/m^2)		SHF(W/m^2)	
	NRA1C	NRA2C	NRA1C	NRA2C
Corr.	0.90	0.93	0.90	0.93
Rms erro	53	48	14	15
Bias	-19	22	-3	-2

Comparing the scatter plots shown in Fig.6 with Fig. 3, it is clear that the latent and sensible heat fluxes are reduced by using COARE 3.0, but the reduction in the NRA1C latent heat loss appears to be too great for latent heat flux values above 200 W/m². Consequently, as shown in Tables 1 and 3, the NRA1C and NRA2C biases are reduced significantly relative to the NRA1 and NRA-2 biases.

Table 5. Correlation coefficients, RMS error, and Bias for each KEO turbulent heat flux component estimated by replacing the given state variable by that from NRA data.

NRA1 LHF	Tair ℃	SST ℃	Qair g/kg	Wind m/s
Corr.	0.99	0.98	0.94	0.96
Rmsd	2	31	64	36
Bias	0	10	-23	-9

NRA2 LHF	Tair ℃	SST ℃	Qair g/kg	Wind m/s
Corr.	0.99	0.98	0.95	0.96
Rmsd	4	39	43	46
Bias	-2	15	-8	13

NRA1 SHF	Tair ℃	SST ℃	Qair g/kg	Wind m/s
Corr.	0.96	0.98	0.99	0.98
Rmsd	12	9	0	9
Bias	-3	2	0	-2

NRA2 SHF	Tair ℃	SST ℃	Qair g/kg	Wind m/s
Corr.	0.95	0.98	0.99	0.98
Rmsd	21	12	0	11
Bias	-9	4	0	3

Table 4. Correlation coefficients, RMS error, and Bias for each turbulent heat flux component of NRA1 adjusted and NRA2 adjusted

	LHF(W/m^2)		SHF(W/m^2)	
	NRA1 Adjusted	NRA2 Adjusted	NRA1 Adjusted	NRA2 Adjusted
Corr.	0.89	0.89	0.93	0.93
Rms erro	71	50	16	14
Bias	-40	-5	-7	-7

Moore and Renfrew (2002) proposed an alternative bulk flux algorithm for NRA data. We also estimate the adjusted turbulent heat fluxes (NRA_Adjusted) by applying their proposed algorithm to NRA data. As shown in the scatter plots of the NRA adjusted fluxes and the KEO buoy turbulent heat fluxes in Fig.7 and in Tables 1 and 4, the adjustment seems to overcorrect NRA1 latent heat flux when the latent heat fluxes is more than 200 W/m².

Another possible cause for the turbulent heat flux errors is errors in the NRA1 state variables. Following Jiang et al. (2005) and Tomita and Kubota (2006) we use daily-averaged state variables from KEO buoy, sequentially replacing the given variable by that from NRA1 and NRA2. The fluxes computed from the daily-mean KEO state variables are the reference flux time series. As shown in Table 5, the accuracy of specific humidity (Qair) is most critical for accurate estimation of NRA1 latent heat flux. The NRA1 latent heat flux RMS error strongly depends upon specific humidity, and to a lesser extent upon wind speed and sea surface temperature. Overall, the Biases and RMS errors due to errors in the state variables are roughly comparable to those due to the algorithm (Tables 3 and 5).

・Conclusions

In this study we have compared the NRA1 surface heat flux data with heat flux data from the new OceanSITES time series reference site surface buoy, KEO, in the Kuroshio Extension recirculation gyre. The error values obtained in this study are considerably larger than those obtained by previous studies. The differences are likely due in part to the buoy location. Because a huge surface heat flux is transferred from the ocean to the atmosphere in the Kuroshio and Kuroshio Extension region it is not surprising that the Bias and Rms error are large compared with other regions. This points to the importance of the KEO buoy and further observations in this region for understanding global climate system. We investigated two possible causes of errors for turbulent heat fluxes: the bulk algorithm and the state variables. The bulk algorithm has substantial influence on the Bias, while errors in state variables mainly affect the Rms errors. The present results point out the importance of maintaining in situ observations that are independent of reanalysis data, and the importance of monitoring surface heat fluxes in the Kuroshio/Kuroshio Extension regions.